Journal of Solid State Chemistry 288 (2020) 121391

Contents lists available at ScienceDirect

Journal of Solid State Chemistry

journal homepage: www.elsevier.com/locate/jssc

A fluorescent titanium-based metal-organic framework sensor for nitroaromatics and nanomolar Fe^{3+} detection

Fangyuan Zhong [a,b,1], Xin Zhang [a,1], Congqin Zheng [a], Hui Xu [a,*], Junkuo Gao [b,**], Shiqing Xu [a,***]

[a] Institute of Optoelectronic Materials and Devices, China Jiliang University, Hangzhou, 310018, China

[b] The Key Laboratory of Advanced Textile Materials and Manufacturing Technology of Ministry of Education, National Engineering Lab for Textile Fiber Materials and Processing Technology (Zhejiang), College of Materials and Textiles, Zhejiang Sci-Tech University, Hangzhou, 310018, China

ARTICLE INFO

Keywords:
Titanium-based metal-organic framework
Metal ions sensing
Nitro-aromatic compounds
Fluorescent test paper
LOD

ABSTRACT

A fluorescent nanoscale titanium-based metal-organic framework materials (MOF), $Ti_6(\mu_3\text{-}O)_6(\mu_2\text{-}OH)_6(BTCA)_2(DMF)_2$ (**ZSTU-3**) was synthesized, with blue fluorescence and delicate conjugated structures indicated its potential as a fluorescence sensor. In this work, we reported a rare example of Ti-MOF for highly sensitive and selective for fluorescence sensing of Fe^{3+} ion and nitro-aromatic compounds. The limit of detection (LOD) for Fe^{3+} ion reaches 70.7 nM and the K_{sv} value is $2.36 \times 10^5\ M^{-1}$, which is among one of the highest LOD values reported by MOFs as far as we known. For the detection of nitro-aromatic compounds, especially 2,4,6-trinitrophenol (PA), the LOD is calculated to be 15.90 μM, and the K_{sv} value is $4.253 \times 10^4\ M^{-1}$. In addition, we also performed a rapid detection of Fe^{3+} ion and nitro-aromatic compounds with fluorescent test paper by naked-eyes. The results demonstrate the superiority of Ti-MOF for detecting Fe^{3+} ion and nitro-aromatic compounds, which may facilitate the detection application in environmental and biological systems.

1. Introduction

Metal-organic frameworks (MOFs), as a fascinating type of porous conjugated multifunctional organic-inorganic hybrid materials [1], have shown many potential applications, such as gas storage and separation [2], catalysis [3], drug delivery [4] and fluorescence sensing [5]. In recent years, it has been widely studied as a kind of luminescent material based on the following advantages [6]: (1) high specific surface area allows sufficient contact between the analytes and MOF, thereby improving the detection sensitivity; (2) the specific functional sites can be specifically identified through host–guest interactions; (3) highly conjugated groups provide good luminescent performance.

Iron is widely distributed in everyday life and the industry, ranking the fourth in the earth's crust content. In addition, iron is also one of the most indispensable elements in the human body [7]. Ferrous ion is an important component of hemoglobin which transports oxygen, and other iron is stored in the liver in the form of ferritin. Excessive or insufficient amount of iron will cause human health problems [8]. On the other hand, nitro-aromatic compounds are compounds in which one or more hydrogen atoms in the benzene ring are replaced by nitro ($-NO_2$), which are usually produced in petrochemical, fuel, paint, explosives and other industries [9]. It is well-known that many nitro-aromatic compounds are harmful substances in the environment, such as nitrobenzene (NB), p-nitrophenol (PNP), 2,4,6-trinitrophenol (PA) and so on, these substances have attracted worldwide attention [10]. Therefore, for the sake of human health and environmental safety, how to detect Fe^{3+} ion and nitro-aromatic compounds in a reliable and convenient way is becoming ever more urgent [11]. To cope with this problem, efforts have been made to detect trace amounts of Fe^{3+} ion and nitro-aromatic compounds with the help of the mass spectrometry (MS), ion mobility spectrometry (IMS), etc., which are of high precision and accuracy but costly and difficult to carry [12]. Therefore, it is crucial to develop an efficient, portable and fast response detection method.

In recent years, the application of nanoscale MOFs and other technologies in detecting metal ions and nitro-aromatic compounds have been rapidly grown [13], which have received widespread attention due to its high detection sensitivity, strong selectivity and fast response time [14]. Particularly, for the Ti(IV) and Zr(IV)-based MOFs, the strong

---

[*] Corresponding author.
[**] Corresponding author.
[***] Corresponding author.

E-mail addresses: huixu@cjlu.edu.cn (H. Xu), jkgao@zstu.edu.cn (J. Gao), shiqingxu75@163.com (S. Xu).

[1] These authors contribute equally to this work.

https://doi.org/10.1016/j.jssc.2020.121391
Received 29 March 2020; Received in revised form 14 April 2020; Accepted 15 April 2020

metal-carboxylic acid bond formed between the high valent metal ions and the organic ligand leads to strong structural rigidity and stability [15]. Restricted by its challenging synthesis, however, only limited Ti-MOFs have been reported and utilized so far [15d]. The pioneering work by Emam group on composites materials based on highly stable MOFs such as MIL-125-NH_2 and UiO-66-$(COOH)_2$ have highlighted the great potential of Ti(IV) and Zr(IV)-based MOFs in catalysis [16]. In previous work, we explored the luminescent sensing properties by NTU-9-NS [17] and ZSTU-1 [8e], and because of whose excellent detection performance for Fe^{3+} and nitro-aromatics, we are committed to explore a novel high efficient Fe^{3+} and nitro-aromatics fluorescence sensor Ti-MOF, with electron-rich triphenylamine ligand, which may lead to efficient electron transfer between MOF and analytes, and thus efficient sensing performance.

In this work, a Ti-MOF $Ti_6(\mu_3\text{-}O)_6(\mu_2\text{-}OH)_6(BTCA)_2(DMF)_2$, (**ZSTU-3;** H_3BTCA = 4′,4‴,4‴’’-nitrilotris([1,1′-biphenyl]-4-carboxylicacid)) with electron-rich triphenylamine ligand was synthesized and explored for the sensing properties. **ZSTU-3** exhibits high sensitivity and selectivity for Fe^{3+} ion and nitro-aromatic compounds, and the detection limit for Fe^{3+} reached to nanomolar level, which is rarely reported.

2. Experimental section

2.1. Materials and general methods

All the chemicals were commercially purchased without further purification. Power X-ray diffraction (PXRD) patterns were recorded on a Bruker D8 Advanced diffractometer with Cu Kα radiation ($\lambda = 1.542$ Å) at a scan rate of 5°/min and a scan range of 3 º– 60°. UV–Vis absorption spectra were obtained on Hitachi U-3900 spectrometer. Fluorescence measurements were obtained from a F-4600 fluorescence spectrometer. The PL lifetime was taken on Fluorolog HORIBA JOBIN YVON. The images of Field Emission Scanning Electron Microscopy (FE-SEM) were recorded on Vltra55, Carl Zeiss. The images of Transmission Electron Microscopy were recorded on JEM-2100.

2.2. Synthesis

2.2.1. Synthesis of ZSTU-3

The **ZSTU-3** was synthesized by hydrothermal method according to the reference [18]. 4′,4‴,4‴’’-nitrilotris([1,1′-biphenyl]-4-carboxylicacid) (H_3BTCA) (400 mg, 0.66 mmol) was dissolved in DMF 5 mL in a 25 mL Teflon-lined stainless-steel autoclave. Treated with ultrasound for 1 h, the clear solution was obtained. During the stirring, titanium isopropoxide (0.16 mL, 0.5 mmol) was added dropwise, and the mixture was a yellow slurry, which then was heated to 180 °C for 30 h. After cooling to room temperature, the mixture was washed with DMF and methanol several times respectively, finally the yellow powder was obtained.

2.3. Metal ions sensing

A series of metal salts solutions (10^{-4} M, metal salts were KNO_3, $AgNO_3$, $Ca(NO_3)_2$, $Mg(NO_3)_2$, $Zn(NO_3)_2$, $Co(NO_3)_2$, $Ni(NO_3)_2$, $Cu(NO_3)_2$, $Fe(NO_3)_3$ respectively) were selected as analytes in fluorescence sensing experiments. Powder of **ZSTU-3** (10 mg) in 100 mL H_2O were sonicated to obtain an aqueous suspension of **ZSTU-3**. The PL spectra was analyzed by adding 50 μL 10^{-4} M metal salts solutions (Ag^+, K^+, Cu^{2+}, Ca^{2+}, Co^{2+}, Zn^{2+}, Ni^{2+}, Mg^{2+}, Fe^{3+}) to 2 mL of **ZSTU-3** aqueous solution.

2.4. Small molecule sensing

A series of organic small molecule analytes (10^{-1} M for H_2O, methanol, acetone, aniline, methylbenzene, DMF, phenol, nitrobenzene, 2,4-DNT, 2,6-DNT, PNP and for 1.22% PA, the concentration of PA was 5.32×10^{-2} M) were selected as analytes in fluorescence sensing experiments. Powder of **ZSTU-3** (10 mg) in 100 mL EtOH were sonicated to obtain an ethanol suspension of **ZSTU-3**. The PL spectra was measured by adding 50 μL ethanol solution of 10^{-1} M organic small molecule (H_2O, methanol, acetone, aniline, methylbenzene, DMF, phenol, nitrobenzene, 2,4-DNT, 2,6-DNT, PNP and 1.22% PA, whose concentration of 1.22% PA is 5.32×10^{-2} M) to 2 mL of **ZSTU-3** ethanol solution.

2.5. The fluorescent photograph of test paper

The experimental filter paper was used as the carrier to prepare the **ZSTU-3** fluorescence sensor. The preparation steps are as follows: the experimental filter paper was cut into a square of 1.5×1.5 cm^2, then soaked in **ZSTU-3** ethanol solution (10 mg/20 mL) for several hours and dried at 60 °C. Fe^{3+} ions and nitro-aromatic compounds were dispersed in aqueous samples (the concentration of 0.122% PA was 5.32×10^{-3} M, and the concentrations of other analytes were consistent with the above headings **2.3** and **2.4**), then dropped on the test paper with pipettes.

3. Results and discussion

The Ti-MOF materials, **ZSTU-3**, was prepared by hydrothermal method according to previously reported reference [18]. The reaction of titanium isopropoxide [$Ti(i\text{-}OPr)_4$] with the ligand H_3BTCA in DMF, which forms a new porous Ti-MOF **ZSTU-3**. The diffraction peaks of the experimental sample were identical to the simulation data, indicating that the synthesized product is a pure phase (Fig. 1). In the **ZSTU-3**, six Ti atoms are participated in a six-connected $Ti_6(\mu_3\text{-}O)_6(COO)_6$ subunit (Fig. 2a), then the Ti_6 clusters are connected via μ_2-OH groups to form an infinite one-dimensional $[Ti_6(\mu_3\text{-}O)_6(\mu_2\text{-}OH)_6(COO)_6]_n$ SBU along the c-axis. In the **ZSTU-3**, the diameter of the elliptical pores along the c-axis is 1.37×0.71 nm, confirming its porous structure (Fig. 2b). The morphology of **ZSTU-3** was observed with transmission electron microscope (TEM) and scanning electron microscope (SEM). Characterization results shown that the sample were nanoparticles with the size of about 50 nm (Fig. 2c and d).

Before the photoluminescence (PL) spectra experiment of **ZSTU-3** material, we tested the fluorescence intensity of the ligand H_3BTCA in the solid state. As shown in Fig. S1, the emission peak of the MOF is similar with that of the ligand, which indicated that the fluorescence performance of **ZSTU-3** can be attributed to the fluorescence emission of the ligand H_3BTCA. According to previous research [18], **ZSTU-3** material exhibited excellent water stability. When dispersed in aqueous and ethanol solution, the emission peaks exhibited slight shift which reached 520 nm and 500 nm, respectively (Fig. S2a and b). In addition, the excellent water stability may be related to the strong coordination bond

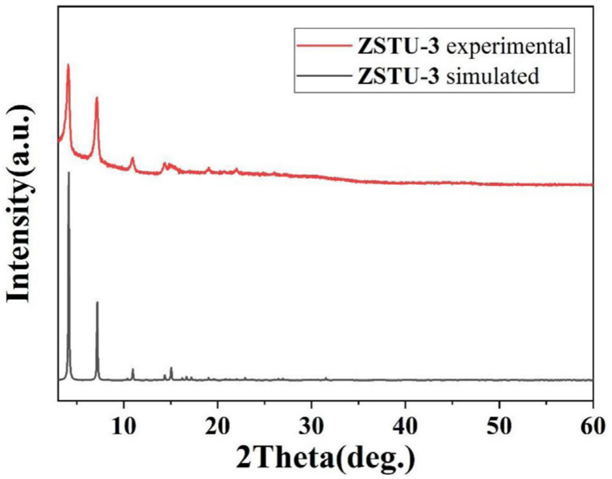

Fig. 1. The experimental and simulated powder XRD patterns of **ZSTU-3**.

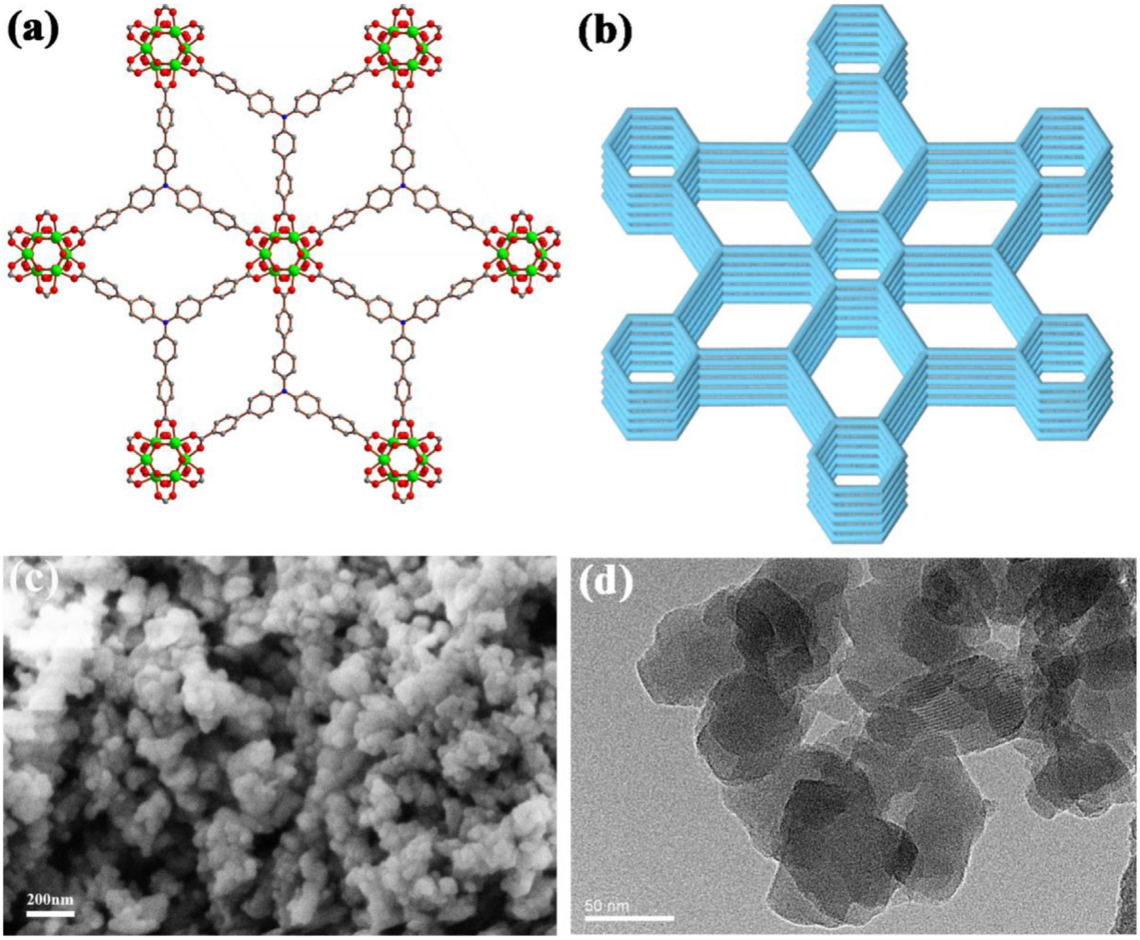

Fig. 2. The structure of (a) along ab plane, (b) 3D porous structure material, (c) The SEM image of **ZSTU-3**, (d) The TEM image of **ZSTU-3**. Color scheme of (a): carbon, black; nitrogen, blue; oxygen, red; metal (Ti), green. (For interpretation of the references to colour in this figure legend, the reader is referred to the Web version of this article.)

between the high valence of Ti(IV) and the ligand with multiple conjugated structures.

Interestingly, addition of small amount of different metal ions (approximately 2.44×10^{-6} mol/L) into the **ZSTU-3** aqueous solution (10 mg **ZSTU-3** dispersed in 100 mL H_2O) produced different degrees of fluorescence quenching (Fig. 3a). Particularly, the adding of Fe^{3+} ion appeared an obvious fluorescence quenching of **ZSTU-3** aqueous solution; while other metal ions almost had no significant effect on the luminescence intensity. Surprisingly, unlike **ZSTU-1**, the quenching effect of Cu^{2+} on the fluorescence intensity of **ZSTU-3** aqueous solution is not obvious as expected, which inspired us to carry out sensing selectivity experiment of **ZSTU-3** aqueous solution. The fluorescence intensity of the **ZSTU-3** aqueous solution can be obviously quenched by adding only 2.44×10^{-6} M of Fe^{3+}, while the fluorescence intensity of the **ZSTU-3** aqueous solution can be almost completely quenched by adding only 4.76×10^{-6} M of Fe^{3+} (Fig. 3b). Interestingly, the blue-shift of fluorescence emission peak occurred at the same time of the fluorescence intensity quenching, which is speculated to be the formation of new metal-organic complexes. Stern-Volmer equation can be used to quantitatively explain the quenching efficiency of Fe^{3+} ions. The relationship between (I_0/I-1) and Fe^{3+} ion concentration can be explained by the Stern-Volmer equation $(I_0/I\text{-}1) = 1 + K_{sv}[Q]$, where I_0 and I are the fluorescence intensity of **ZSTU-3** and the fluorescence intensity of **ZSTU-3** after adding Fe^{3+} ion, respectively, [Q] represents the concentration of Fe^{3+} ion. The K_{sv} curve of Fe^{3+} was linear in the low concentration range, and the K_{sv} value was 2.36×10^5 M^{-1} (Fig. 3c). The limit of detection for Fe^{3+} ion was calculated to be 70.7 nM (Fig. S3), which is one of the highest values reported for MOF-based Fe^{3+} ion fluorescence sensors (Table S1).

In addition, we further investigated the sensing performance of **ZSTU-3** in ethanol solution for organic small molecules. As shown in Fig. 4a, the addition of different small molecules into the **ZSTU-3** ethanol solution will produce different degrees of fluorescence quenching, the concentration of small molecules is 2.44×10^{-3} mol/L whereas the concentration of PA is 1.30×10^{-3} mol/L. It is worth noting that the **ZSTU-3** material has different fluorescence quenching effects towards different nitro-aromatic molecules. The **ZSTU-3** ethanol solution was almost completely quenched after adding 9.09×10^{-4} M p-nitrophenol (PNP), while the fluorescence quenching effect of 2,4-dinitrotoluene (2,4-DNT) and 2,6-dinitrotoluene (2,6-DNT) was slightly less effective. The fluorescence intensity of the **ZSTU-3** ethanol solution was only quenched by about a quarter after adding nitrobenzene (NB) with the same concentration (Fig. S4). Interestingly, the fluorescence intensity of **ZSTU-3** ethanol solution was also almost completely quenched after adding only 4.84×10^{-4} M 2,4,6-trinitrophenol (PA) (Fig. 4b). The order of the quenching effect of different nitro-aromatic molecules is PA > PNP>2,4-DNT≈2,6-DNT > NB. This order is in accordance with the trend of electron-withdrawing groups [19]. The above results show that among nitro-aromatic molecules, PA exhibits the most significant fluorescence quenching effect on **ZSTU-3** ethanol solution. **ZSTU-3** ethanol solution has a linear correlation with PA concentration in the low concentration range. Similarly, the quenching efficiency of PA can also be quantitatively explained by using the Stern-Volmer equation, and the K_{sv} value was 4.253×10^4 M^{-1} (Fig. 4c). The limit of detection for PA was

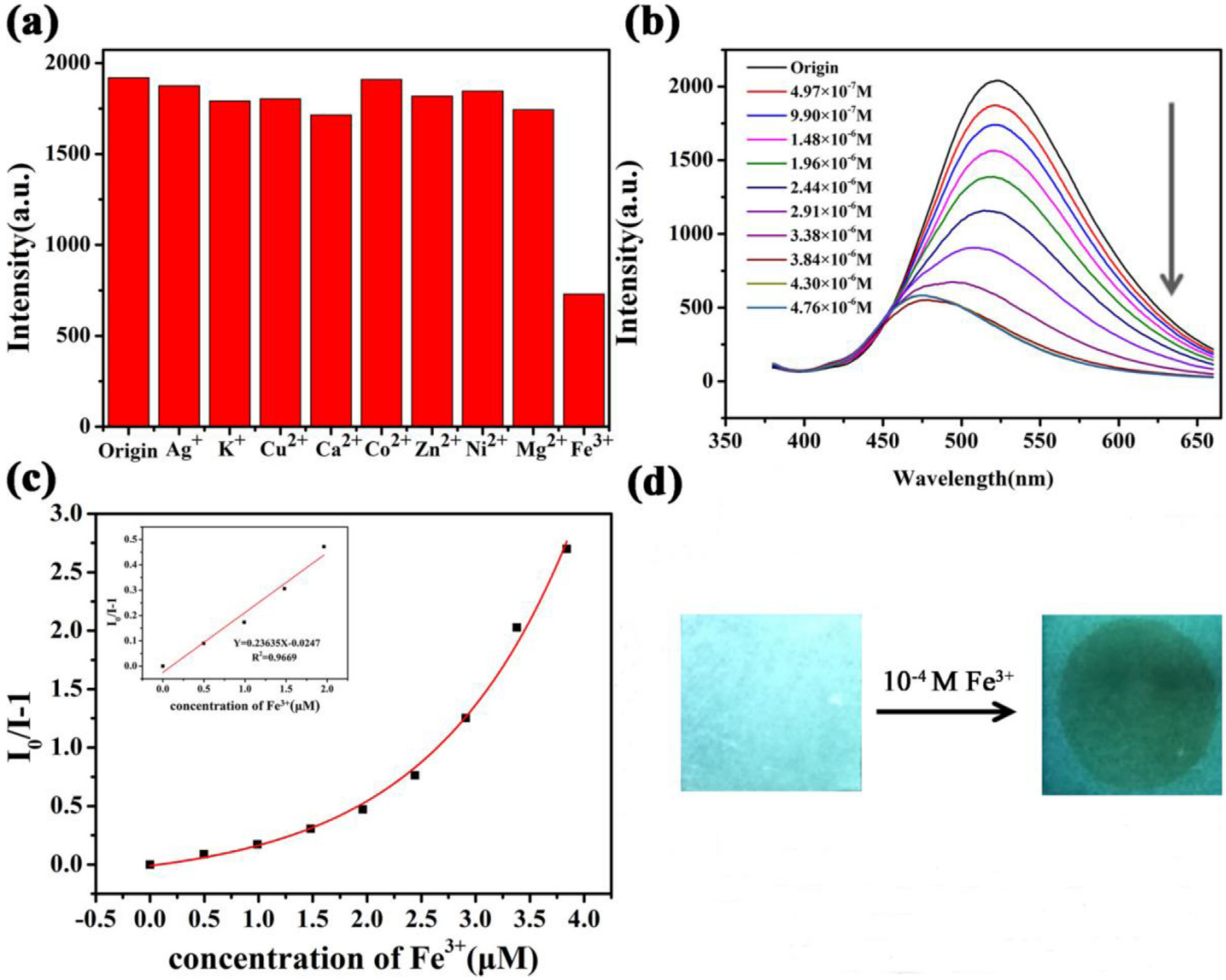

Fig. 3. (a) Fluorescence intensity of 5 × 10^{-9} mol different metal ions added to **ZSTU-3** aqueous solution at 520 nm emission, (b) The **ZSTU-3** PL spectra with different amounts of Fe^{3+} ion, (c) The SV curve of Fe^{3+}, inset: the quenching fluorescence upon addition of 2 μM Fe^{3+}, (d) Photograph of fluorescence response after 5 μL, 10^{-4} M of Fe^{3+} ion was added to test paper under 365 nm UV light.

calculated to be 15.90 μM (Fig. S5), which are better than some previous report (Table S2).

PXRD was carried out to examine the structural stability upon addition of different analytes. As shown in Fig. S6, PXRD was examined with **ZSTU-3** materials soaked in Fe^{3+}, NB, 2,4-DNT, 2,6-DNT, PNP and PA for 24 h, respectively. The results show that the XRD patterns of **ZSTU-3** powders soaked in different analytes solutions remained the same, exhibiting the structural stability of **ZSTU-3** materials. As shown in Fig. S7, patterns of the FT-IR of **ZSTU-3** before and after addition of different analytes were identical, which indicates no new chemical bond is formed. The fluorescence lifetime of **ZSTU-3** before and after the addition of the analytes were almost the same, indicating that there was no coordination bond between **ZSTU-3** and the analytes (Fig. S8, Table S3 and S4).

In order to investigate the fluorescence quenching mechanism of **ZSTU-3** materials after adding Fe^{3+} ions and nitro-aromatic compounds, the UV absorption spectra of different metal ions/nitro-aromatic compounds and **ZSTU-3** and the emission spectra of **ZSTU-3** was tested. As shown in Fig. S10, in the range of 300–400 nm, the UV–Vis absorption spectra of Fe^{3+} ions in aqueous solution and PA in ethanol solution shown stronger UV–Vis absorption and larger overlap with the emission spectra of **ZSTU-3**. The effective overlap between the emission spectra of the **ZSTU-3** material and the absorption spectra of nitro-aromatic compounds and Fe^{3+} ions indicates that a fluorescence resonance energy transfer (FRET) [20] process may occur during the fluorescence quenching process (Fig. S10), this spectral overlap may cause part of the energy generated by the electronic transition in the **ZSTU-3** material to be directly transferred to the analytes, instead of emitting fluorescence in the form of radiative transitions, resulting in a decrease in fluorescence intensity. Also, considering the strong electron withdrawn ability of Fe^{3+} ions and nitro-aromatic molecules, the fluorescence quenching can also be attributed to the photoinduced electron transfer (PET) process [17, 21]. In summary, both electron transfer and energy transfer may contribute to the effective fluorescence quenching of **ZSTU-3** materials by Fe^{3+} ions and nitro-aromatic compounds.

Finally, a fluorescent paper test was performed. **ZSTU-3** fluorescent test paper emits bright blue light under ultraviolet (365 nm) irradiation, while when a spot of Fe^{3+} ion aqueous solution and PA ethanol solution were dropped onto the fluorescent test paper, the blue fluorescence changed to dark immediately (Figs. 3d and 4d). The results indicate that the potential of **ZSTU-3** in a fast fluorescence and visible to the naked eye detection of Fe^{3+} ion and nitro-aromatic molecules.

4. Conclusions

A fluorescent titanium-based MOF (**ZSTU-3**) nanoparticles was synthesized exhibited highly selective and sensitive sensing towards Fe^{3+} ion and nitro-aromatic compounds through adding different analytes.

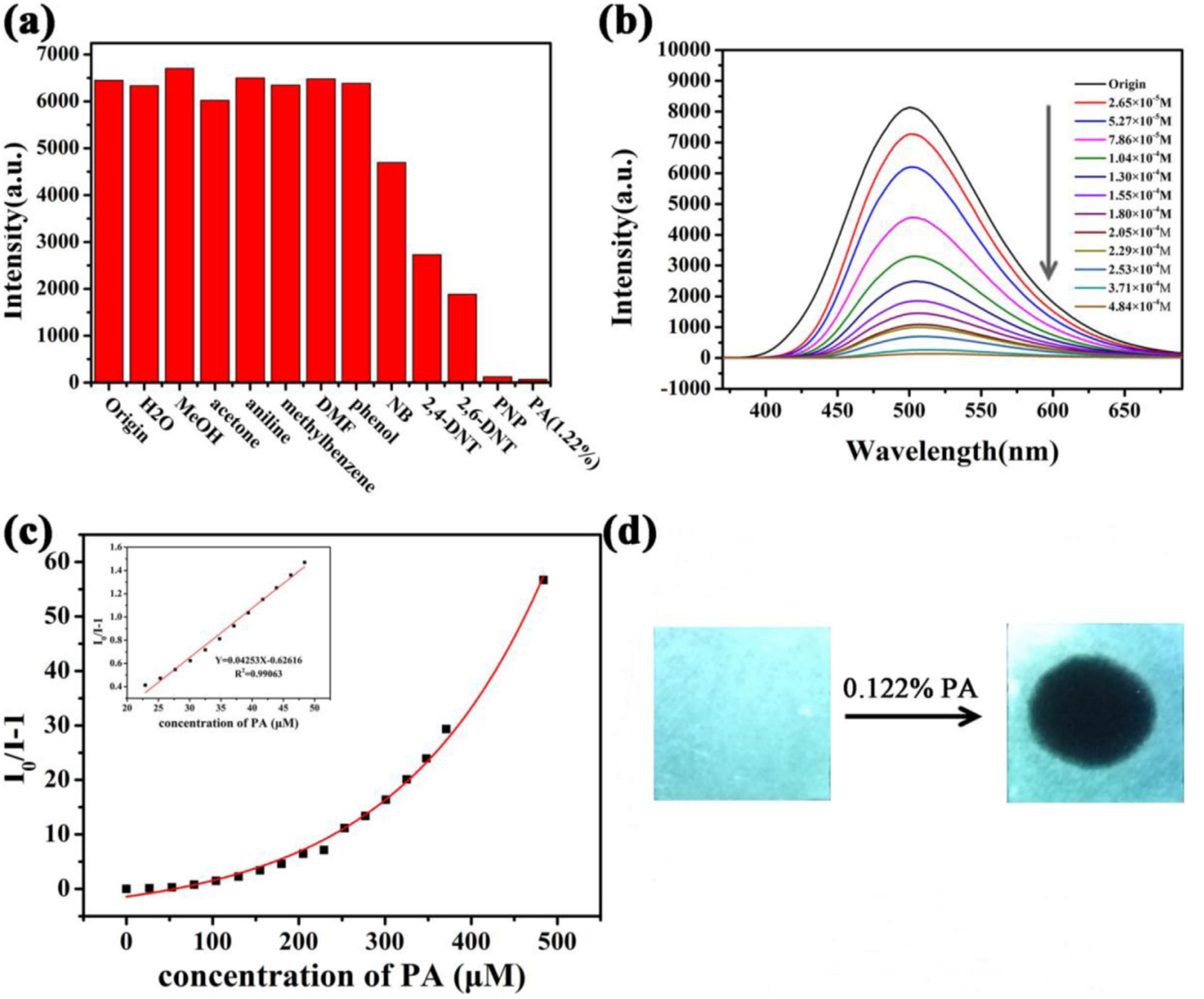

Fig. 4. (a) Fluorescence intensity of 5 × 10^{-6} mol different organic small molecule (among them, the amount of PA was 2.66 × 10^{-6} mol) added to **ZSTU-3** ethanol solution at 500 nm emission, (b) The **ZSTU-3** PL spectra under different amounts of PA, (c) The SV curve of PA, inset: the quenching fluorescence upon addition of 50 μM PA, (d) Photograph of fluorescence response after 5 μL, 0.122% PA was added to test paper under 365 nm UV light.

The **ZSTU-3** exhibits high detection limit towards Fe^{3+} ion and PA, with the value reached 70.7 nM and 15.90 μM, respectively. Both electron transfer and energy transfer contribute to the effective fluorescence quenching of **ZSTU-3** material. This result demonstrates that Ti-MOF, as a multi-response fluorescent probe, exhibits potential application in detecting metal ions and nitro-aromatic compounds, and provides a feasible way to utilize porous Ti-MOFs on fluorescent sensors in the environment and biological areas.

Declaration of competing interest

The authors declare that they have no known competing financial interests or personal relationships that could have appeared to influence the work reported in this paper.

CRediT authorship contribution statement

Fangyuan Zhong: Writing - original draft. **Xin Zhang:** Methodology. **Congqin Zheng:** Formal analysis. **Hui Xu:** Supervision. **Junkuo Gao:** Supervision. **Shiqing Xu:** Supervision.

Acknowledgements

This work was supported by Natural Science Foundation of Zhejiang Province (No. LY19E020007). J. G. acknowledges the financial support from the Fundamental Research Funds of Zhejiang Sci-Tech University (2019Q007).

Appendix A. Supplementary data

Supplementary data to this article can be found online at https://doi.org/10.1016/j.jssc.2020.121391.

References

[1] a) J. Kim, B. Chen, T.M. Reineke, H. Li, M. Eddaoudi, D.B. Moler, M. O'Keeffe, O.M. Yaghi, Assembly of Metal−Organic frameworks from large organic and inorganic secondary building Units: new examples and simplifying principles for complex structures, J. Am. Chem. Soc. 123 (2001) 8239–8247;
b) H. Li, M. Eddaoudi, M. O'Keeffe, O.M. Yaghi, Design and synthesis of an exceptionally stable and highly porous metal-organic framework, Nature 402 (1999) 276–279;
c) M. Eddaoudi, H. Li, O.M. Yaghi, Highly porous and stable Metal−Organic Frameworks: structure design and sorption properties, J. Am. Chem. Soc. 122 (2000) 1391–1397;

d) J.L.C. Rowsell, O.M. Yaghi, Metal–organic frameworks: a new class of porous materials, Microporous Mesoporous Mater. 73 (2004) 3–14;
e) Y. Li, T. Zhao, M. Lu, Y. Wu, Y. Xie, H. Xu, J. Gao, J. Yao, G. Qian, Q. Zhang, Enhancing oxygen evolution reaction through modulating electronic structure of trimetallic electrocatalysts derived from metal-organic frameworks, Small 15 (2019) 1901940;
f) Y. Li, M. Lu, Y. Wu, H. Xu, J. Gao, J. Yao, Trimetallic metal-organic framework derived carbon-based nanoflower electrocatalysts for efficient overall water splitting, Adv. Mater. Interfaces 6 (2019) 1900290.

[2] a) J.L. Rowsell, E.C. Spencer, J. Eckert, J.A. Howard, O.M. Yaghi, Gas adsorption sites in a large-pore metal-organic framework, Science 309 (2005) 1350–1354;
b) A.I. Skoulidas, D.S. Sholl, Self-diffusion and transport diffusion of light gases in metal-organic framework materials assessed using molecular dynamics simulations, J. Phys. Chem. B 109 (2005) 15760–15768;
c) Z. Zhang, Y. Zhao, Q. Gong, Z. Li, J. Li, MOFs for CO2 capture and separation from flue gas mixtures: the effect of multifunctional sites on their adsorption capacity and selectivity, Chem. Commun. 49 (2013) 653–661;
d) J.-R. Li, Y. Ma, M.C. McCarthy, J. Sculley, J. Yu, H.-K. Jeong, P.B. Balbuena, H.-C. Zhou, Carbon dioxide capture-related gas adsorption and separation in metal-organic frameworks, Coord. Chem. Rev. 255 (2011) 1791–1823;
e) J.L.C. Rowsell, O.M. Yaghi, Strategies for hydrogen storage in metal–organic frameworks, Angew. Chem. Int. Ed. 44 (2005) 4670–4679;
f) A.R. Millward, O.M. Yaghi, Metal−Organic frameworks with exceptionally high capacity for storage of carbon dioxide at room temperature, J. Am. Chem. Soc. 127 (2005) 17998–17999;
g) J. Gao, X. Qian, R.-B. Lin, R. Krishna, H. Wu, W. Zhou, B. Chen, Mixed metal-organic framework with multiple binding sites for efficient C2 H2/CO2 separation, Angew. Chem. Int. Ed. 59 (2020) 4396–4400;
h) R.-B. Lin, H. Wu, L. Li, X.-L. Tang, Z. Li, J. Gao, H. Cui, W. Zhou, B. Chen, Boosting ethane/ethylene separation within isoreticular ultramicroporous metal–organic frameworks, J. Am. Chem. Soc. 140 (2018) 12940–12946;
i) M. Shao, Y. Cheng, T. Zhang, S. Li, W. Zhang, B. Zheng, J. Wu, W.-W. Xiong, F. Huo, J. Lu, Designing MOFs-derived FeS2@Carbon composites for high-rate sodium ion storage with capacitive contributions, ACS Appl. Mater. Interfaces 10 (2018) 33097–33104.

[3] a) Y.K. Hwang, D.Y. Hong, J.S. Chang, S.H. Jhung, Y.K. Seo, J. Kim, A. Vimont, M. Daturi, C. Serre, G. Ferey, Amine grafting on coordinatively unsaturated metal centers of MOFs: consequences for catalysis and metal encapsulation, Angew. Chem. Int. Ed. 47 (2008) 4144–4148;
b) I. Luz, F.X. Llabrés i Xamena, A. Corma, Bridging homogeneous and heterogeneous catalysis with MOFs: "Click" reactions with Cu-MOF catalysts, J. Catal. 276 (2010) 134–140;
c) A. Dhakshinamoorthy, H. Garcia, Catalysis by metal nanoparticles embedded on metal-organic frameworks, Chem. Soc. Rev. 41 (2012) 5262–5284;
d) A.H. Chughtai, N. Ahmad, H.A. Younus, A. Laypkov, F. Verpoort, Metal–organic frameworks: versatile heterogeneous catalysts for efficient catalytic organic transformations, Chem. Soc. Rev. 44 (2015) 6804–6849;
e) W. Ren, J. Gao, C. Lei, Y. Xie, Y. Cai, Q. Ni, J. Yao, Recyclable metal-organic framework/cellulose aerogels for activating peroxymonosulfate to degrade organic pollutants, Chem. Eng. J. 349 (2018) 766–774;
f) J.-N. Zhu, X.-Q. Zhu, F.-F. Cheng, P. Li, F. Wang, Y.-W. Xiao, W.-W. Xiong, Preparing copper doped carbon nitride from melamine templated crystalline copper chloride for Fenton-like catalysis, Appl. Catal. B Environ. 256 (2019) 117830.

[4] a) C.-Y. Sun, C. Qin, X.-L. Wang, Z.-M. Su, Metal-organic frameworks as potential drug delivery systems, Expet Opin. Drug Deliv. 10 (2013) 89–101;
b) S.R. Miller, D. Heurtaux, T. Baati, P. Horcajada, J.-M. Grenèche, C. Serre, Biodegradable therapeutic MOFs for the delivery of bioactive molecules, Chem. Commun. 46 (2010) 4526–4528;
c) L.-L. Tan, H. Li, Y. Zhou, Y. Zhang, X. Feng, B. Wang, Y.-W. Yang, Zn2+-Triggered drug release from biocompatible zirconium MOFs equipped with supramolecular gates, Small 11 (2015) 3807–3813;
d) R.C. Huxford, J. Della Rocca, W. Lin, Metal–organic frameworks as potential drug carriers, Curr. Opin. Chem. Biol. 14 (2010) 262–268.

[5] a) H.-L. Jiang, Y. Tatsu, Z.-H. Lu, Q. Xu, Non-, micro-, and mesoporous Metal−Organic framework isomers: reversible transformation, fluorescence sensing, and large molecule separation, J. Am. Chem. Soc. 132 (2010) 5586–5587;
b) M.M. Wanderley, C. Wang, C.-D. Wu, W. Lin, A chiral porous metal–organic framework for highly sensitive and enantioselective fluorescence sensing of amino alcohols, J. Am. Chem. Soc. 134 (2012) 9050–9053;
c) B. Liu, W.-P. Wu, L. Hou, Y.-Y. Wang, Four uncommon nanocage-based Ln-MOFs: highly selective luminescent sensing for Cu2+ ions and selective CO2 capture, Chem. Commun. 50 (2014) 8731–8734;
d) Y. Lu, B. Yan, A ratiometric fluorescent pH sensor based on nanoscale metal–organic frameworks (MOFs) modified by europium(iii) complexes, Chem. Commun. 50 (2014) 13323–13326;
e) H. Xu, Y. Dong, Y. Wu, W. Ren, T. Zhao, S. Wang, J. Gao, An -OH group functionalized MOF for ratiometric Fe3+ sensing, J. Solid State Chem. 258 (2018) 441–446.

[6] F.-Y. Yi, D. Chen, M.-K. Wu, L. Han, H.-L. Jiang, Chemical sensors based on metal–organic frameworks, ChemPlusChem 81 (2016) 675–690.

[7] J.L. Bricks, A. Kovalchuk, C. Trieflinger, M. Nofz, M. Büschel, A.I. Tolmachev, J. Daub, K. Rurack, On the development of sensor molecules that display FeIII-amplified fluorescence, J. Am. Chem. Soc. 127 (2005) 13522–13529.

[8] a) C.-X. Yang, H.-B. Ren, X.-P. Yan, Fluorescent metal–organic framework MIL-53(Al) for highly selective and sensitive detection of Fe3+ in aqueous solution, Anal. Chem. 85 (2013) 7441–7446;
b) S. Dang, E. Ma, Z.-M. Sun, H. Zhang, A layer-structured Eu-MOF as a highly selective fluorescent probe for Fe3+ detection through a cation-exchange approach, J. Mater. Chem. 22 (2012) 16920–16926;
c) Z. Xiang, C. Fang, S. Leng, D. Cao, An amino group functionalized metal–organic framework as a luminescent probe for highly selective sensing of Fe3+ ions, J. Mater. Chem. A. 2 (2014) 7662–7665;
d) X.-Y. Xu, B. Yan, Eu(III)-Functionalized MIL-124 as fluorescent probe for highly selectively sensing ions and organic small molecules especially for Fe(III) and Fe(II), ACS Appl. Mater. Interfaces 7 (2015) 721–729;
e) F. Zhong, C. Li, Y. Xie, H. Xu, J. Gao, Titanium metal-organic framework nanorods for highly sensitive nitroaromatic explosives detection and nanomolar sensing of Fe3+, J. Solid State Chem. 278 (2019) 120892.

[9] B. Gole, A.K. Bar, P.S. Mukherjee, Fluorescent metal–organic framework for selective sensing of nitroaromatic explosives, Chem. Commun. 47 (2011) 12137–12139.

[10] a) D. Tian, Y. Li, R.-Y. Chen, Z. Chang, G.-Y. Wang, X.-H. Bu, A luminescent metal–organic framework demonstrating ideal detection ability for nitroaromatic explosives, J. Mater. Chem. A. 2 (2014) 1465–1470;
b) J. Qin, B. Ma, X.-F. Liu, H.-L. Lu, X.-Y. Dong, S.-Q. Zang, H. Hou, Aqueous- and vapor-phase detection of nitroaromatic explosives by a water-stable fluorescent microporous MOF directed by an ionic liquid, J. Mater. Chem. A. 3 (2015) 12690–12697;
c) Y.-N. Gong, L. Jiang, T.-B. Lu, A highly stable dynamic fluorescent metal–organic framework for selective sensing of nitroaromatic explosives, Chem. Commun. 49 (2013) 11113–11115.

[11] Z. Zhang, S. Xiang, X. Rao, Q. Zheng, F.R. Fronczek, G. Qian, B. Chen, A rod packing microporous metal–organic framework with open metal sites for selective guest sorption and sensing of nitrobenzene, Chem. Commun. 46 (2010) 7205–7207.

[12] a) G.A. Eiceman, J.A. Stone, Peer reviewed: ion mobility spectrometers in national defense, Anal. Chem. 76 (2004) 390 A–397 A;
b) B.J.A. Berendsen, R.S. Wegh, T. Meijer, M.W.F. Nielen, The assessment of selectivity in different quadrupole-orbitrap mass spectrometry acquisition modes, J. Am. Soc. Mass Spectrom. 26 (2015) 337–346.

[13] a) C. Li, J. Hai, S. Li, B. Wang, Z. Yang, Luminescent magnetic nanoparticles encapsulated in MOFs for highly selective and sensitive detection of ClO−/SCN− and anti-counterfeiting, Nanoscale 10 (2018) 8667–8676;
b) Y. Cui, B. Chen, G. Qian, Lanthanide metal-organic frameworks for luminescent sensing and light-emitting applications, Coord. Chem. Rev. 273–274 (2014) 76–86;
c) L. Zhang, Z. Kang, X. Xin, D. Sun, Metal–organic frameworks based luminescent materials for nitroaromatics sensing, CrystEngComm 18 (2016) 193–206;
d) H. Xu, X. Rao, J. Gao, J. Yu, Z. Wang, Z. Dou, Y. Cui, Y. Yang, B. Chen, G. Qian, A luminescent nanoscale metal–organic framework with controllable morphologies for spore detection, Chem. Commun. 48 (2012) 7377–7379;
e) X. Zhang, F. Zhong, J. Liu, H. Xu, J. Gao, S. Xu, A new three-dimensional metal-organic framework based on dinuclear rare earth cluster and olsalazine, Z. Anorg. Allg. Chem. 645 (2019) 1267–1270;
f) L. Wang, H. Xu, J. Gao, J. Yao, Q. Zhang, Recent progress in metal-organic frameworks-based hydrogels and aerogels and their applications, Coord. Chem. Rev. 398 (2019) 213016.

[14] a) J. Wang, X. Qian, J. Cui, Detecting Hg2+ ions with an ICT fluorescent sensor Molecule: remarkable emission spectra shift and unique selectivity, J. Org. Chem. 71 (2006) 4308–4311;
b) Y. Ma, H. Su, X. Kuang, X. Li, T. Zhang, B. Tang, Heterogeneous nano metal–organic framework fluorescence probe for highly selective and sensitive detection of hydrogen sulfide in living cells, Anal. Chem. 86 (2014) 11459–11463;
c) S. Wu, Y. Lin, J. Liu, W. Shi, G. Yang, P. Cheng, Rapid detection of the biomarkers for carcinoid tumors by a water stable luminescent lanthanide metal–organic framework sensor, Adv. Funct. Mater. 28 (2018) 1707169.

[15] a) T. Devic, C. Serre, High valence 3p and transition metal based MOFs, Chem. Soc. Rev. 43 (2014) 6097–6115;
b) C. Wang, Y.-H. Luo, X.-T. He, D.-L. Hong, J.-Y. Wang, F.-H. Chen, C. Chen, B.-W. Sun, Porous high-valence metal–organic framework featuring open coordination sites for effective water adsorption, Inorg. Chem. 58 (2019) 3058–3064;
c) M. Kandiah, M.H. Nilsen, S. Usseglio, S. Jakobsen, U. Olsbye, M. Tilset, C. Larabi, E.A. Quadrelli, F. Bonino, K.P. Lillerud, Synthesis and stability of tagged UiO-66 Zr-MOFs, Chem. Mater. 22 (2010) 6632–6640;
d) J. Zhu, P.-Z. Li, W. Guo, Y. Zhao, R. Zou, Titanium-based metal–organic frameworks for photocatalytic applications, Coord. Chem. Rev. 359 (2018) 80–101.

[16] a) R.M. Abdelhameed, H.R. el-deib, F.M.S.E. El-Dars, H.B. Ahmed, H.E. Emam, Applicable strategy for removing liquid fuel nitrogenated contaminants using MIL-53-NH2@Natural fabric composites, Ind. Eng. Chem. Res. 57 (2018) 15054–15065;
b) R.M. Abdelhameed, H.E. Emam, Design of ZIF(Co & Zn)@wool composite for efficient removal of pharmaceutical intermediate from wastewater, J. Colloid Interface Sci. 552 (2019) 494–505;
c) R.M. Abdelhameed, M. Rehan, H.E. Emam, Figuration of Zr-based MOF@cotton fabric composite for potential kidney application, Carbohydr. Polym. 195 (2018) 460–467;
d) H.E. Emam, A.E. Abdelhamid, R.M. Abdelhameed, Refining of liquid fuel from N-Containing compounds via using designed Polysulfone@Metal organic framework composite film, J. Clean. Prod. 218 (2019) 347–356;
e) H.E. Emam, H.N. Abdelhamid, R.M. Abdelhameed, Self-cleaned photoluminescent viscose fabric incorporated lanthanide-organic framework (Ln-MOF), Dyes Pigments 159 (2018) 491–498;
f) H.E. Emam, H.B. Ahmed, H.R. El-Deib, F.M.S.E. El-Dars, R.M. Abdelhameed, Non-invasive route for desulfurization of fuel using infrared-assisted MIL-53(Al)-NH2 containing fabric, J. Colloid Interface Sci. 556 (2019) 193–205;

g) H.E. Emam, H.B. Ahmed, E. Gomaa, M.H. Helal, R.M. Abdelhameed, Doping of silver vanadate and silver tungstate nanoparticles for enhancement the photocatalytic activity of MIL-125-NH2 in dye degradation, J. Photochem. Photobiol. Chem. 383 (2019) 111986.

[17] H. Xu, J. Gao, X. Qian, J. Wang, H. He, Y. Cui, Y. Yang, Z. Wang, G. Qian, Metal–organic framework nanosheets for fast-response and highly sensitive luminescent sensing of Fe3+, J. Mater. Chem. A. 4 (2016) 10900–10905.

[18] C. Li, H. Xu, J. Gao, W. Du, L. Shangguan, X. Zhang, R.-B. Lin, H. Wu, W. Zhou, X. Liu, J. Yao, B. Chen, Tunable titanium metal–organic frameworks with infinite 1D Ti–O rods for efficient visible-light-driven photocatalytic H2 evolution, J. Mater. Chem. A. 7 (2019) 11928–11933.

[19] Z. Hu, B.J. Deibert, J. Li, Luminescent metal–organic frameworks for chemical sensing and explosive detection, Chem. Soc. Rev. 43 (2014) 5815–5840.

[20] X. Zhang, Y. Xiao, X. Qian, A ratiometric fluorescent probe based on FRET for imaging Hg2+ ions in living cells, Angew. Chem. Int. Ed. 47 (2008) 8025–8029.

[21] a) P.L. Feng, K. Leong, M.D. Allendorf, Charge-transfer guest interactions in luminescent MOFs: implications for solid-state temperature and environmental sensing, DTr 41 (2012) 8869–8877;
b) M. Gutierrez, B. Cohen, F. Sánchez, A. Douhal, Photochemistry of Zr-based MOFs: ligand-to-cluster charge transfer, energy transfer and excimer formation, what else is there? Phys. Chem. Chem. Phys. 18 (2016) 27761–27774.